Modelling of the Target Voltage Behaviour in Reactive Sputtering

R. De Gryse*, D. Depla
University Ghent, Krijgslaan 281/S1, B-9000 GENT, Belgium

Abstract

It has been shown that at least two mechanisms are responsible for target poisoning during reactive sputtering, i.e. sub plantation of the reactive gas ions underneath the target surface and chemisorption on the target surface. At first sight, both processes may look quite similar however their influence on the target poisoning is very different. Also with respect to the absolute target (ATV) voltage behaviour the differences are very pronounced. The reason for these differences finds its origin in the fact that sub planted species can react with the target metal and form compound molecules, or can remain unreacted as dissolved reaction gas in the target. It has been shown that the dissolved reaction gas leads to an increase in ATV.
The formed compound, for instance the oxide, at the target surface and subsurface behaves completely different with respect to the ATV as compared to target material onto which reaction gas has been chemisorbed. This has to do with the difference between the ion induced secondary electron emission (ISEE) coefficient of the formed oxide as compared to the ISEE coefficient of the target material partly covered with chemisorbed oxygen. Moreover, chemisorption on oxide, formed by sub plantation, is nearly impossible.
A model is discussed in which the ATV is expressed as the weighted difference between the fraction of the target surface area occupied by chemisorbed species and the fraction of the target surface which is converted into compound by ion implantation. This model is used to understand the ATV behaviour during reactive sputtering of aluminium in an argon/oxygen mixture. At high pumping speeds and/or low sputter currents, a substantial increase in ATV is observed for oxygen flows smaller than the critical flow which drives the target in complete poisoning. For higher flows than the critical flow, chemisorption reduces the sputtering speed and leverages the sub plantation effect which drives the target into poisoning. The corresponding drop in ATV is essentially due to sub plantation and the corresponding formation of aluminium oxide together with a reduction of the plasma impedance due to the pressure increase. At low pumping speeds and/or high currents, i.e. when wall gettering is important, chemisorption on the target and its effect on the ATV is greatly reduced due to the competition between sub plantation and chemisorption.

1. Introduction

It is generally accepted that during reactive sputtering the target voltage is controlled by two effects namely a plasma effect and the variation of the Ion-induced Secondary Electron Emission (ISEE) coefficient. The first effect has to do with the variation of the plasma impedance under the influence of variations in sputter partial pressures of the sputter gas and reactive gas when going from metallic sputtering toward poisoning. The second and dominating effect is due to the formation of a compound layer at the target surface, a compound layer which has a different ISEE value as compared to the bare target surface. While the first effect leads to a slow decrease of the target voltage the ISEE-effect is characterized by abrupt variations of the target voltage in a narrow region of pressure or flow variations. This article will essentially focus on the effect of the ISEE-coefficient on the absolute target voltage (ATV).
During the reactive sputtering process, the partial pressure of the reactive gas is lowered by the chemical reaction between the reactive gas and the sputtered target material. This is the so-called gettering process. This process is generally described by chemisorption of the reactive gas on the target material deposited on the substrate and the chamber walls[1]. Of course, this reaction can also occur on the target but there the sputtering process balances it. The balance between sputtering and chemical reaction on the

*Corresponding author: Tel.: +32-9-264 4342; fax: +32-9-264 4996
E-mail address: Roger.Degryse@ugent.be (R. De Gryse)

target changes towards more chemical reaction when the flow rate of the reactive gas exceeds the getter rate. This reduces the erosion rate of the target because the formed compound sputters less efficiently than the original target material. Consequently, the getter rate reduces further resulting in an avalanche situation and an abrupt change in the partial pressure of the reactive gas, which is mostly accompanied with an abrupt change in target voltage and deposition rate. This description of the reactive sputtering process is summarized in the model of Berg et.al.[1] As shown by the authors[2], even for reactive gas/target combinations where gettering plays an important role, i.e. O_2/Al, chemisorption alone can not explain the measured target voltage behaviour and ion implantation plays also an important role in the poisoning mechanism during the reactive sputtering process. Therefore, a model was put forward [9] which is an extended version of the model, proposed by Berg et.al.[1], taking into account the effect of ion implantation. In this way, it becomes possible to describe the reactive sputtering process irrespective of the used reactive gas/target combination.
Based on this model it is shown that the variation in ATV, when driving the target in poisoning, can be simulated with good accuracy by using the difference between the effective fraction of the target covered by chemisorption θ_{tc}^{*} and the fraction θ_{ti} of the target surface that has reacted with the subplanted reactive atoms under the formation of compound.

2. Experimental

The experimental conditions have been previously described in detail [3]. For the target voltage experiments the same set-up was used. However, to investigate the influence of the pumping speed a valve was introduced between the vacuum chamber and the turbomolecular pump. We have used a Hüttinger 1500 DC power supply in constant current mode. The pumping speed was measured by using the ratio between the measured flow (MKS type 246) and the measured argon pressure (MKS Baratron).

3. Overview of the model

Figure 1 gives a schematic overview of the extended model. Similar to the model proposed by Berg et.al. [1]we define three reactive gas flows : i) the reactive gas flow to the target q_t, ii) the reactive gas flow to the substrate q_s and iii) the reactive gas flow to the pump q_p. The total of these flows is equal to the reactive gas flow introduced in the chamber, q_o. The reactive gas molecules can chemisorb on the substrate (and chamber walls), resulting in a given fraction θ_{sc} of the substrate which has reacted. The reactive gas ions become implanted into the target, resulting in a given degree of reaction for the target θ_{ti}, as described in the first part of the paper. On the non-reacted part of the target ($1-\theta_{ti}$), reactive gas molecules can chemisorb on the target surface, resulting in an effective fraction of the target covered by chemisorbed molecules

$$\theta_{ti}^{*} = \theta_{ti}\left(1-\theta_{ti}\right) \qquad (1)$$

Without going into the mathematical details (which can be found in ref. 10) and assuming steady state conditions, the extended model is governed by a set of equations given in the appendix.
It follows that starting from experimental values of the discharge current density I, the total gas pressure P_T and the partial pressure P of the reaction gas, all relevant quantities pertaining to the target can be calculated.
At the substrate and chamber walls only chemisorption is the mechanism at play and has been fully documented by Berg et al. [1]. The variation in time of the chemisorbed fraction on the substrate (and walls) θ_{sc} is given by

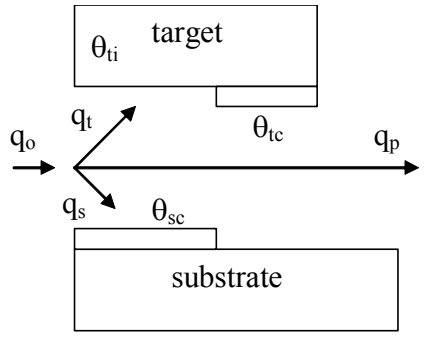

Figure 1. Overview of the extended model. See text for a detailed description of the different symbols.

$$n_{opp}\frac{d\theta_{sc}}{dt}=\frac{2\alpha_{sc}}{a}(1-\theta_{sc})F + I\gamma_R\left[(1-\theta_{ti})\theta_{tc}+\theta_{ti}\left(\frac{n_o}{n_o+N}\right)\right](1-\theta_{sc})\frac{A_t}{A_s} - I\gamma_M(1-\theta_{ti})(1-\theta_{tc})\left(\frac{n_o}{n_o+N}\right)\theta_{sc}\frac{A_t}{A_s} \quad (9)$$

with A_t and A_s the respective areas of target racetrack and substrate, α_{sc} the sticking coefficient of the reaction gas on the freshly deposited target material and n_{opp} the target surface density. It should be noted that the influence of shallow implantation on the target is taken into account by the factors containing θ_{ti} and $(1-\theta_{ti})$. In steady state conditions the left hand side of equation (9) equals zero which allows one to calculate θ_{sc} which in turn gives access to the respective gas flows towards substrate and target.

$$q_s=\frac{RT}{N_a}\alpha_{sc}(1-\theta_{sc})F.A_s \quad (10)$$

$$q_t=\frac{RT}{N_a}\alpha_{tc}(1-\theta_{tc})(1-\theta_{ti})FA_t+\frac{fI}{N_a}RTA_t \quad (11)$$

Taking into account the gas flow transferred by the pump

$$q_p=P.S \quad (12)$$

with S the pumping speed, the total gas flow q_o of the reaction gas is given by

$$q_o=q_p+q_s+q_t \quad (13)$$

and allows us to discuss variations of ATV as a function of the flow of reaction gas. In the following paragraph we will first discuss the different parameters needed for describing the system Al/O_2 i.e. aluminium sputtered reactivily in a mixture of Argon and oxygen.

For the pumping speed S and the ion current density I, the experimental values described in figure 2 and 3 were used. Also the experimental value of the argon pressure (0.2 Pa) was used. The racetrack area A_t (10^{-2} m^2) was measured from a sputtered target. We have set the substrate surface area (and chamber walls) A_s to 1 m^2. We have assumed that the formed compound on the target by ion implantation or chemisorption is Al_2O_3, i.e. a = 1.5. The sputter yield for Al (0.5) was calculated from SRIM 2000.40 [4]. For the sputter yield of Al_2O_3 we have used the experimental value of 0.03[5]. In our calculation, we have neglected the weighting of the sputter yield by the mole fraction f for the bombardment by Ar^+

and R_2^+ ions because for the performed experiments (see further) the reactive gas mole fraction in the plasma is always small.

The reaction probability α_{ti} has been set equal to 1 as it is generally accepted that the implanted oxygen atoms have a high affinity for the target material. As shown by the authors [1] there is evidence for the presence of non-reacted oxygen in the target before complete poisoning. As was discussed in ref. [9] this can be attributed to the high current density used during magnetron sputtering. Indeed, at this high current density the rate-determining step in the reaction is not the supply of oxygen atoms to the target, as it is the case during ion beam experiments. Therefore, when the target is partially poisoned, some of the oxygen can remain in the target without chemical reaction. As shown by the authors [2], when the magnetron is switched off, these non-reacted oxygen atoms will react further with the target material or desorb from the target as oxygen molecules. We have used the same values for β and N_{max} as in the case of Si/N_2 (see ref. 9), although no experimental evidence for these values can be given. However, and as mentioned before, the value of β and N_{max} does not affect the general behaviour of the calculated results.

From the simulations, we have noticed that the most important parameters are the sticking coefficients needed to describe the chemisorption on the target and the substrate. A best fit between the experimental target voltage curves and the calculated ones (see further) has been achieved using a value of 0.03 and 0.2, respectively for the sticking coefficient on the target α_{tc} and on the substrate α_{sc}. The higher sticking coefficient for chemisorption on the substrate than on the target can be attributed to the higher activity of the deposited aluminium. A similar reasoning has been used to explain the higher sticking coefficient on freshly evaporated Ti films [6]. The sticking coefficient on the substrate is in the same order of magnitude than the reported sticking coefficient reported by Kusano et.al. on Ti substrates during reactive sputtering of Ti in Ar/O_2[6]. The sticking coefficient on the target is 10 times larger than the value of the sticking coefficient (0.003) as measured by the authors for O_2 on a freshly sputtered target [5]. However, in the latter situation the sticking coefficient was measured in the power-off mode of the magnetron. As shown by Pekker [7], the dissociation of molecular oxygen in the plasma during magnetron sputtering can be significant. As the produced oxygen atoms have a high sticking coefficient on aluminium, the average sticking coefficient will be larger than the sticking coefficient for molecular oxygen on the aluminium target and will depend on the degree of dissociation of the molecular oxygen. As the degree of dissociation of molecular oxygen is small before full oxidation of the target, or under conditions of high pumping speed[7], the used value of the sticking coefficient is reasonable.

Most published models assume for the sticking coefficient on the target α_{tc} and on the substrate α_{sc} a value of 1. This value can only be reached under reactive sputtering conditions where the degree of dissociation of the molecular gas is very high [7].

In our approach we assume that the bombardment of the target with the reactive gas ions depends linearly on the mole fraction of the reactive gas in the plasma, neglecting the plasma chemistry.

4. Simulation of the absolute target voltage (ATV)

To describe the target voltage behaviour as a function of the oxygen flow, the influence of the different poisoning mechanisms, i.e. chemisorption and reactive ion implantation, on the target voltage must be known. It is generally accepted that Al_2O_3 has a larger ISEE coefficient than Al. Therefore, the formation of bulk oxide due to reactive ion implantation will influence the target voltage. An increase of the ISEE coefficient of the target will result in a smaller absolute value of the target voltage when the current is kept constant. As shown by the authors, chemisorption of oxygen on an aluminium target [2][5], reduces the ISEE coefficient and is accompanied with an increase of the absolute target voltage until one monolayer of oxygen is chemisorbed. Therefore, we have used the sum $(w_{tc}\theta_{tc}^{*}-w_{tc}\theta_{ti})$ to compare the calculated values with the measured target voltage behaviour. In this sum w_{tc} and w_{ti} represent two weighting coefficients which have been set to 1 as no data is available on the magnitude of the target voltage decrease due to bulk oxidation by ion implantation. θ_{tc}^{*} represent the effective fraction of the target covered by chemisorption and is calculated from

$$\theta_{tc}^{*} = \theta_{tc}\left(1-\theta_{ti}\right) \tag{8}$$

and, as discussed before, results in an increase of the absolute target voltage.

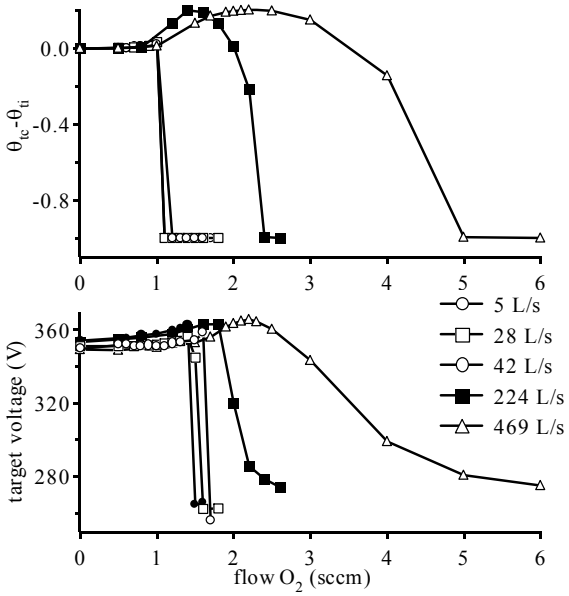

Fig. 2. (a)Behaviour of the target condition as a function of the oxygen flow using the parameters described in the text.
(b) Behaviour of the target voltage as a function of oxygen flow. For these experiments the current as kept constant at 200 mA and the pumping speed was varied. The argon pressure as kept constant for all experiment at Pa and oxygen was added to the plasma

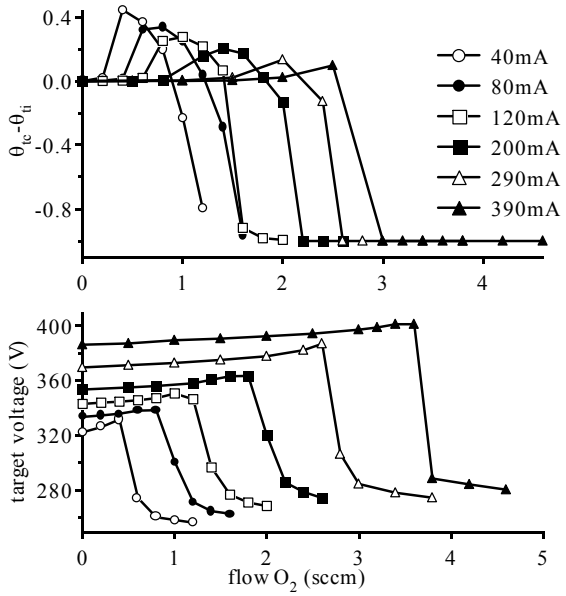

Fig 3. (a) Behaviour of the target condition as a function of the oxygen flow using the parameters described in the text
(b) Behaviour of the target voltage as a function of the oxygen flow. For these experiments the pumping speed was kept constant at 224 L/s. The argon pressure was kept constant for all experiments at 0.2 Pa and oxygen was added to the plasma.

The target voltage will also decrease by the sudden pressure increase when the gettering of oxygen is reduced. However, this sudden pressure increase is always accompanied with the full oxidation of the target, which is described by θ_{ti} and in this way this effect has already taken into account.
In figure 2 and 3 we show the target voltage behaviour as a function of the oxygen flow for two different experimental series. In this first series, we have varied the pumping speed while in the second series the current was varied. Also the calculated values of ($w_{tc}\theta_{tc}^{*}$-$w_{ti}\theta_{ti}$) (with $w_{tc} = w_{t\,i}=1$) are shown. In both series we notice that the calculated results show a similar behaviour as the experimental results. The experiments show that the small target voltage rise, noticed before the abrupt drop of the target voltage, becomes smaller for lower pumping speeds and higher currents. This behaviour is reflected by the calculations. Figure 4 shows the behaviour of both θ_{tc}^{*} and θ_{ti} a function of the oxygen flow for two different pumping speeds. This figure 4 clearly demonstrates that the target voltage must increase due to chemisorption and then will decrease due to the bulk oxidation by reactive ion implantation. The effect is much more pronounced at high pumping speed then at low pumping speed.
This behaviour of the target condition can be understood as follows. When the flow rate of the reactive gas exceeds the getter rate at approximately 1 sccm of reactive gas, the effective reactive gas partial pressure starts to increase. At high pumping speed (or at low current) this pressure increase is quite small in contrast to the low pumping speed (or high current) experiments. Therefore, the reactive gas mole fraction f is quite small. As chemisorption is directly proportional with the partial pressure (see equation (7)), chemisorption plays initially a more important role than reactive ion implantation in the poisoning mechanism. The chemisorption of reactive gas on the target surface, reduces, however the target surface recession speed or the erosion rate of the target. In this way, reactive ion implantation becomes more pronounced. As the reactive gas does not chemisorbs on the reacted target surface, the effect of chemisorption is reduced. At low pumping speed (or high current) the increase of the reactive gas partial

pressure is much stronger and in this way the reactive gas mole fraction becomes large enough to fully oxidise the target by reactive ion implantation.

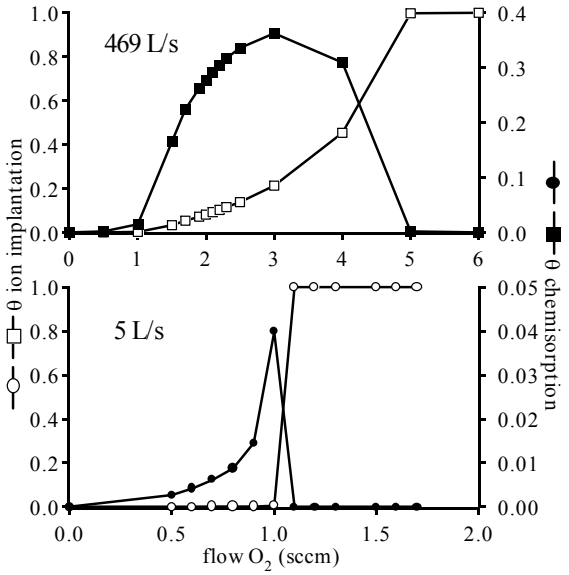

Figure 4. θ_{tc}* (closed symbols, right hand axis) and θ_{ti} (open symbols left hand axis) as a function of the oxygen flow (different X-axis scale) for two different pumping speeds (and constant current of 200 mA).

5. Conclusion

By correlating the absolute target voltage (ATV) with the effective covered fraction of the target by chemisorption θ_{tc}^{*} minus the fraction θ_{ti} of the target surface converted into compound by subplantation of reaction gas, a fairly good agreement between the experimental observed variation of the ATV versus the flow of reaction gas and the calculated values is obtained. Comparing the influence of chemisorption with the influence of implantation, shows that even in systems, such as Al/O_2 sputtering, in which poisoning has been attributed traditionally to chemisorption, this effect alone is not able to describe the observed ATV values during poisoning. Indeed, even in those systems, chemisorption is essentially a trigger for the real poisoning mechanism, namely, reactive subplantation.

Appendix

The relevant equations (10) describing the extended model are:

$$\theta_{ti} = 1 - \exp - \left[\left(\frac{\alpha_n}{a} \right) \cdot \left(\frac{n}{n_o} \right) \right] \tag{2}$$

$$n = \frac{2f}{Y} \cdot n_o \tag{3}$$

$$N = N_{max} \left\{ 1 - \exp - \frac{\beta \cdot n}{N_{max}} \cdot \left[1 - \alpha_{ti} \left(1 - \theta_{ti} \right) \right] \right\} \tag{4}$$

$$Y = \gamma_m \left(1 - \theta_{ti} \right) \left(1 - \theta_{tc} \right) \frac{n_o}{n_o + N} + \gamma_R \left[\left(1 - \theta_{ti} \right) \theta_{tc} \frac{n_o}{n_o + N} \right] \tag{5}$$

$$2\frac{\alpha_{tc}F}{a}(1-\theta_{tc})-I\gamma_R\theta_{tc}=0 \quad (6)$$

$$F=\frac{PN_a}{\sqrt{2\pi MRT}} \quad (7)$$

$$f=\frac{P}{P_T} \quad (8)$$

The symbols are defined as follows:

θ_{tc}: fraction of target surface covered by chemisorption

θ_{ti}: fraction of target surface that has reacted with subplanted reactive atoms or ions under the formation of compound

n: concentration of subplanted reactive gas atoms before reaction and diffusion (m^{-3})

n_o: target density (m^{-3})

α_{ti}: reaction probability of a subplanted atom with a target lattice atom

a: number of reactive gas atoms needed to form one molecule of the compound

f: mole fraction of the reactive gas in the gas phase

Y: sputter yield of the target

N: concentration of subplanted and non reacted ions in the target (m^{-3})

N_{max}: Maximum value of N (m^{-3})

γ_M: sputter yield of the target material

γ_R: sputter yield of the compound

α_{tc}: sticking coefficient of reactive gas molecules on the target

F: flux of reactive gas molecules towards the target (at. $m^{-2}.s^{-1}$)

I: discharge current density (ions $m^{-2}.s^{-1}$)

β: probability that a subplanted reactive atom remains non reached in the target

P_T: total pressure (P_a)

P: partial pressure of reaction gas (P_a)

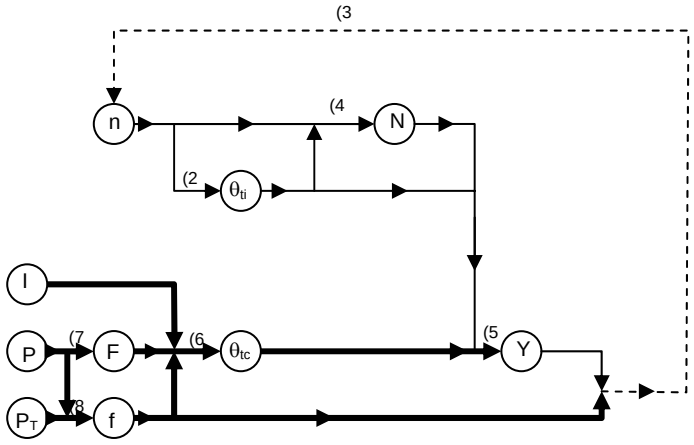

Fig. A1 shows the flow chart for calculating all relevant quantities. The numbers between brackets refer to the corresponding equations. Bold lines show that part of the flow chart that is directly accessible from the experimental quantities I, P and P_T. It allows to calculate F, f and θ_{tc}. Thin lines show the iterative part of the flow chart. Starting with a best guess for n, it allows to calculate a new value of n. Feeding back this value (hatched line) starts an iterative process until initial and final values of n are converging. This gives calculated values for θ_{ti}, θ_{sc} and N.

References

[1] S. Berg, H.-O. Blom, T. Larsson, C. Nender, J. Vac. Sci. Technol. A5(2) (1987) 202-207
[2] D. Depla, R. De Gryse, Plasma Sources Sci. Technol. 10 (2001) 547-555
[3] D. Depla, A. Colpaert, K. Eufinger, A. Segers, J. Haemers, R. De Gryse, Vacuum 66 (2002) 9-17
[4] J.F. Ziegler, J.P. Biersack, L. Littmark, The stopping and Range of Ions in Solids, Pergamon, New York (1985); SRIM can be downloaded from http://www.srim.org
[5] D. Depla, R. De Gryse, J. Vac. Sci. Technol. A20(2) (2002) 521-525
[6] E. Kusano, S. Baba, A. Kinbare, J. Vac. Sci. Technol. A10(4) (1992) 1696-1700
[7] L. Pekker, Thin Solid Films 312 (1998) 341-347
[8] D. Depla, A. Colpaert, K. Eufinger, A. Segers, J. Haemers, R. De Gryse, Vacuum 66 (2002) 9-17
[9] D. Depla, R. De Gryse, Surface and Coatings Technology 183 (2004) 190-195

CLICK TO RETURN TO LIST OF PAPERS AND PRESENTATIONS